Two-step phase-shift interferometry with known but arbitrary reference waves: a graphical interpretation

Nail Sabitov,[1,*] Thomas Meinecke,[1] Damien P. Kelly,[2] and Stefan Sinzinger[1]

[1]Institut für Mikro- und Nanotechnologien, Fachgebiet Technische Optik, Technische Universität Ilmenau, PF 100565, Ilmenau, Thüringen 98684, Germany

[2]Institut für Mikro- und Nanotechnologien, Fachgebiet Optik-Design, Modellierung und Simulation optischer Systeme, Technische Universität Ilmenau, PF 100565, Ilmenau, Thüringen 98684, Germany

*Corresponding author: nail.sabitov@tu-ilmenau.de

Received 7 June 2012; revised 19 August 2012; accepted 20 August 2012; posted 21 August 2012 (Doc. ID 170178); published 0 MONTH 0000

There are many applications in biology and metrology where it is important to be able to measure both the amplitude and phase of an optical wave field. There are several different techniques for making this type of measurement, including digital holography and phase retrieval methods. In this paper we propose an analytical generalization of this two-step phase-shifting algorithm. We investigate how to reconstruct the object signal if both reference waves are different in phase and amplitude. The resulting equations produce two different solutions and hence an ambiguity remains as to the correct solution. Because of the complexity of the generalized analytical expressions we propose a graphical-vectorial method for solution of this ambiguity problem. Combining our graphical method with a constraint on the amplitude of the object field we can unambiguously determine the correct result. The results of the simulation are presented and discussed. © 2012 Optical Society of America

OCIS codes: 090.2880, 110.2960, 120.2880, 120.3180.

1. Introduction

The reconstruction of the phase and amplitude distribution of an object wavefront is useful for a variety of applications, such as biology or material science. There it allows one to examine/measure the homogeneity of transparent materials, such as glass and plastics. Most methods for determining the phase and amplitude distributions of an object signal are based on interferometry. We start with a review and classification of the most widespread techniques in this area.

The main problem of classical off-axis holography is the limited spatial resolution of the reconstructed complex object signal. As is shown in [1] the maximum spatial frequency of the reconstructed object wavefront should not exceed one-quarter of the camera sampling rate. At the same time only one frame is needed for a signal recovery in off-axis interferometry.

The so-called slightly off-axis method [1,2] allows one to increase the maximum spatial frequency resolved in the object signal to one-half of the detector sampling rate by decreasing the angle between object and reference wave. In this case the central auto correlation zero-order term overlaps with the off-axis real and virtual subspectra. Thus, two intensity recordings are necessary to retrieve the object wavefront unambiguously. In conventional slightly off-axis method the two interferograms should be recorded with different relative phase shifts between the reference wave and the constant phase of the object wave. This is realized by a controlled delay of the reference beam. This technique is similar to classical

1559-128X/12/286831-08$15.00/0

phase-shifting interferometry. Therefore, the method is often designated as two-step phase-shifting interferometry.

It is possible to capture two recordings sequentially [1] or simultaneously separated in space. Different techniques for capturing of two interferograms simultaneously using a single CCD camera [2–5]. The in-line interferometry method allows one to estimate the complex value of the object wavefront with the pixel resolution in the detector plane. At least three intensities have to be recorded for this method with different delays of the reference wave. Therefore, the capturing of dynamic processes is challenging. For implementation of parallel phase-shifting interferometry sophisticated phase retarding array devices are used [6,7]. In [8] an interesting method using the Talbot effect for producing regularly reference field with different phase steps is described. The authors implement the method for capturing of color holograms.

By four-exposure quadrature phase-shifting holography [9–11] four recordings should be taken for the reconstruction. These recordings are two interference pattern, object, and reference waves intensities. The three-exposure quadrature phase-shifting holography means that one takes the same recording excepting object wave intensity. If only two interference patterns are captured the method is called two-exposure quadrature phase-shifting holography. In this case phase and intensity distribution of the reference wave should be premeasured. The authors in [12] compare two-, three-, and four-exposure phase-shifting holography. They stated that the quality of two- and three-exposure holograms is identical. The object wave intensity has maximum limitation. If intensity ratio of object and reference waves increases, the quality of two- and three-exposure holograms becomes lower because of noise. The four-exposure hologram does not have this drawback of object wave intensity limitation.

The challenging method of two-step-only phase-shifting or quadrature interferometry allows reconstruction of the complex object field from only two intensity recordings. The price for this significant advantage is a restricted dynamic range of object wave intensity and the necessity for premeasuring of the reference wave intensity [2,13].

Various mathematical approaches were presented in applications of two-phase step phase-shifting interferometry (PSI) [2,5,7,9,10,13–17] for suppressing of undesirable zero-order and twin-image components. Another interesting method for zero-order- and twin-image-less reconstruction of single-exposure interferograms was proposed in [16]. The zero-order elimination carried out by nonlinear logarithmical processing with assumption that the object wave should be weaker than the reference wave. Extraction of side order occurs by using Hilbert phase-shifting interference. In some algorithms [7,14] the reference wave delay is fixed to $\delta = \pi/2$. In this case the reconstruction algorithm can become simpler [7]. In [18], the authors used the approach of the often cited "The general theory of phase-shifting algorithms" [17] to resolve the problem of unknown phase shifting by two-step-only PSI. In [19], the authors suppose a method for rotating of the reference wave phase by adjusting of the amplitude ratio of two coherent pi/2 shifted components of the reference wave.

In this article we generalize the two-step phase-shifting interferometry method. In the proposed method both interferograms can be taken with reference waves arbitrary both in phase and in amplitude. For retrieving the complex object signal according to the algorithm presented in the second section we need to know two intensities of reference waves as well as the phases of both reference waves before the capturing of both holograms. The challenge of this algorithm is ambiguity. This ambiguity results when trying to find an analytical solution for the general case. A restriction of the object wave is one way to resolve this problem. In the third section we suggest a new graphical vector approach to define the necessary requirements for the object wave to be restored. In the fourth section we present simulation confirming the proposed method. We finish with a short conclusion.

2. Theoretical Analysis

First, we define the experimental situation we model analytically. The principle of the interferogram capturing is schematically illustrated in Fig. 1. The beam splitter BS ensures that the unknown complex object wave A_O at the planes of both detectors D_1 and D_2 is the same. Each detector is also illuminated by a reference wave. The two reference waves at the planes of detectors D_1 and D_2 are characterized by complex distributions U_{R1} and U_{R2}, respectively. The detectors D_1 and D_2 capture the interference intensities I_1 and I_2. Suppose that arbitrary reference waves U_{R1} and U_{R2} are known in phase and amplitude at the moment of the recording of the interferograms I_1 and I_2 by the detectors. Importantly the

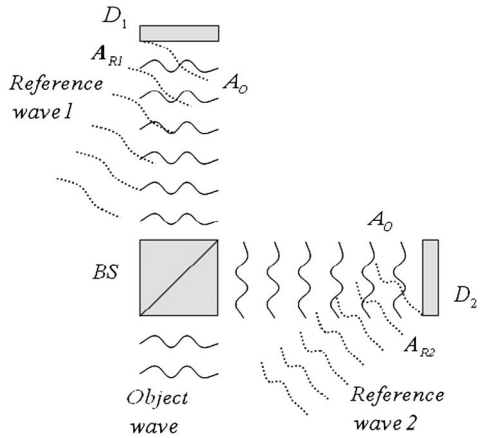

Fig. 1. Experimental setup illustrated schematically. D_1 and D_1, matrix detectors; A_O, unknown complex amplitude of object wave; A_{R1} and A_{R2}, complex amplitude distributions of two arbitrary reference waves; BS, beam splitter.

object wave A_O and reference waves U_{R1} and U_{R2} are coherent. So the phase difference between U_{R1} and U_O or between U_{R2} and U_O remains stable during the recording. The equations in Eq. (1) are conventional interference equations and present the dependence of the captured intensities I_1 and I_2 by the detectors D_1 and D_2 resulting from the interference of the complex functions U_{R1} and U_O (for intensity I_1) or U_{R2} and U_O (for intensity I_2).

The object wave $\{I_O, \phi_O\}$ (in complex form $U_O = [I_O]^{1/2}\exp(i\varphi_O)$) can be found out by solving the set (1) of two interference equations analytically;

$$\begin{cases} I_1 = I_{R1} + I_O + 2\sqrt{I_{R1}}\sqrt{I_O}\,\cos(\varphi_{R1} - \varphi_O) \\ I_2 = I_{R2} + I_O + 2\sqrt{I_{R2}}\sqrt{I_O}\,\cos(\varphi_{R2} - \varphi_O) \end{cases}, \tag{1}$$

where I_1 and I_2 are intensities of captured interferograms; I_O and φ_O are the intensity and phase of the object wave; I_{R1}, φ_{R1}, I_{R1}, and φ_{R2} are intensities and phases of two reference waves.

Since the solution is quite complex for the arbitrary reference waves, the detail is presented in Appendix A. Here we present the final solution as quadratic equation for I_O and a set of two equations for the phase:

$$\begin{aligned} &\left[I_{R1} + I_{R2} - 2\,\cos(d)\sqrt{I_{R1}I_{R2}}\right]I_O^2 \\ &+ \left[2\,\cos(d)(J_2 + J_1)\sqrt{I_{R1}I_{R2}} - 2J_1I_{R2} - 2J_2I_{R1}\right. \\ &\left. - 4\sin^2(d)I_{R1}I_{R2}\right]I_O + J_1^2I_{R2} \\ &- 2\,\cos(d)J_1J_2\sqrt{I_{R1}I_{R2}} + J_2^2I_{R1} = 0, \end{aligned} \tag{2}$$

where $d = \varphi_{R1} - \varphi_{R2}$, $J_1 = I_1 - I_{R1}$, and $J_2 = I_2 - I_{R2}$.

This equation is solved as conventional quadratic equation and has two intensity roots I'_O and I''_O for the object wave. Solving of set of Eq. (3) yields the phase φ'_O related to the intensity I'_O. For calculating the phase for the second object wave φ''_O the intensity I''_O should be set in the same set of Eq. (3) instead of I'_O:

$$\begin{cases} \varphi'_O = \varphi_{R1} \pm \arccos\left(\frac{I_1 - I_{R1} - I'_O}{2\sqrt{I_{R1}I'_O}}\right) \\ \varphi'_O = \varphi_{R2} \pm \arccos\left(\frac{I_2 - I_{R2} - I'_O}{2\sqrt{I_{R2}I'_O}}\right) \end{cases}. \tag{3}$$

Finally, object wave can be represented in complex distributions like $U'_O = [I'_O]^{1/2}\exp(i\varphi'_O)$ and $U''_O = [I''_O]^{1/2}\exp(i\varphi''_O)$. So an ambiguity (duality of the solution) arises in trying to find out the original object wave. This ambiguity consists due to the presence of one false root among U'_O and U''_O. But it is impossible to conclude without *a priori* information which of the two roots (U'_O or U''_O) corresponds to the correct object wave. It is important to note that both possible complex object signals U'_O and U''_O are real physical complex values. In [5] the duality was solved analytically because of the simplified assumption of equal amplitudes for both reference waves ($U_{R1} = U_{R2}$). It was found that the object wave must be weaker than the reference wave for true reconstruction. In our case the derived expressions for recovering of the object intensity I'_O, I''_O [Eq. (2)] and phase φ'_O, φ''_O [Eq. (3)] in the case of arbitrary reference wave amplitudes ($U_{R1} \neq U_{R2}$) are too complex to process them analytically. Nevertheless they [Eqs. (2) and (3)] can be applied for numerical reconstructions after appropriate simplification. Because of the complexity of the analytical expressions we suggest a graphical approach for resolving the ambiguity problem and for clear description of this phenomenon.

3. Graphical Approach

The objects of the graphical approach are vectors in the complex plane. Let us reformulate the set [Eq. (1)] into the form of complex vector values [Eq. (4)]:

$$\begin{cases} \bar{U}_1 = \bar{U}_{R1} + \bar{U}_O \\ \sqrt{I_1} = |\bar{U}_1| \\ \bar{U}_2 = \bar{U}_{R2} + \bar{U}_O \\ \sqrt{I_2} = |\bar{U}_2| \end{cases}. \tag{4}$$

The introduced complex values $\bar{U}_1$ and $\bar{U}_2$ define the complex sum disturbances in the plane of the detectors D_1 and D_2 (see Fig. 1). The magnitudes of $\bar{U}_1$ and $\bar{U}_2$ are equal to the square root of the signal intensities I_1 and I_2. The reference disturbances $\bar{U}_{R1}$ and $\bar{U}_{R2}$ should be known. All these values are defined for one specific spatial location in the object field. The task is to find the complex object distribution $\bar{U}_O$.

Now we show how to find the solution of the equation set [Eq. (4)] graphically. The presented vector conditions [Fig. 2(a)] are only one example. The graphical representation of the first equation $\bar{U}_1 = \bar{U}_{R1} + \bar{U}_O$ [Eq. (4)] is typically a vector triangle. In our case the vector $\bar{U}_O$ will tense between the end points of $\bar{U}_{R1}$ and $\bar{U}_1$. The initial points of $\bar{U}_1$ and $\bar{U}_{R1}$ are located in the coordinate origin. The second equation $\sqrt{I_1} = |\bar{U}_1|$ [Eq. (4)] implies that the magnification of the sum disturbance $|\bar{U}_1|$ is defined. Because of the unknown phase of the $\bar{U}_1$ it is only possible to determine the vector family for the object vector $\bar{U}_O$ [Fig. 2(a)] being a solution for first two equations in the set [Eq. (4)]. Each vector of this family begins from reference vector $\bar{U}_{R1}$ and has its end point at the circle c_1 with radius $|\bar{U}_1|$. The same considerations are valid for the second pair of equations [Eq. (4)], which yields second vector family [Fig. 2(b)].

The solution of the equation set [Eq. (4)] is such vector $\bar{U}_O$, which has the same length and direction in both vector arrays [Figs. 2(a) and 2(b)]. To graphically find this solution we push the two drawings [Figs. 2(a) and 2(b)] until the sense points of reference

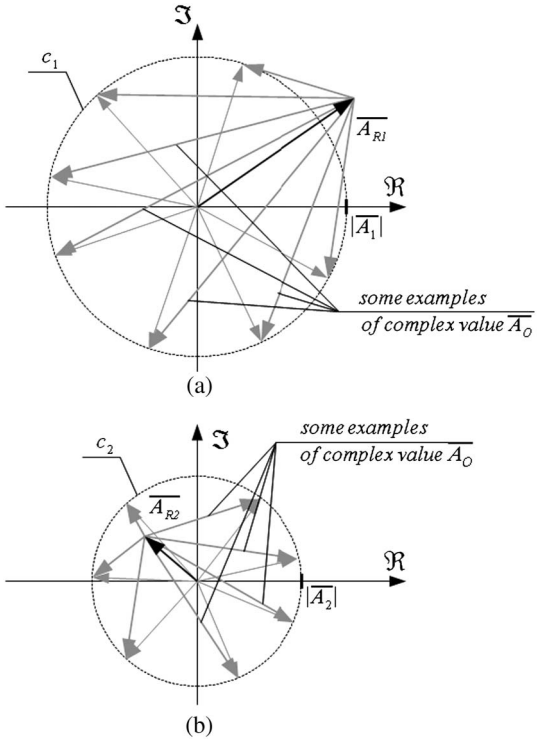

Fig. 2. Graphical vectorial illustration of Eq. (4) at the complex plane for some possible values of the object value. (a) Illustration of some possible values which are an answer to Eqs. (4a) and (4b). (b) Illustration of some possible values which are an answer to Eqs. (4c) and (4d). $\bar{A}_{R1}$ is a known reference complex value, $\bar{A}_O$object complex value, c_1 is a circle with radius $|\bar{A}_1| = [I_1]^{1/2}$ and center at the coordinate origin. c_2 is a circle with radius $|\bar{A}_1| = [I_1]^{1/2}$ and center at the coordinate origin.

vectors $\bar{U}_1$ and $\bar{U}_2$ coincide in point R (Fig. 3). The intersection points of circles (Fig. 3) P' and P'' correspond to the two solutions of the equation set [Eq. (4)] $\bar{U}'_O$ and $\bar{U}''_O$. This pair of solutions is equal to the analytical solution of [Eqs. (2) and (3)]. This graphical approach will help us to solve the ambiguity problem described in the previous section.

Suppose the sequence of experiments is carried out with different object waves. The reference disturbances $\bar{U}_{R1}$ and $\bar{U}_{R2}$ should remain unchanged and known during these experiments. It means that points O_1, O_2 and R as well as straight line will not change the position O_1O_2. Changing of $\bar{U}_O$ each experiment will cause to displacement points P' and P'',

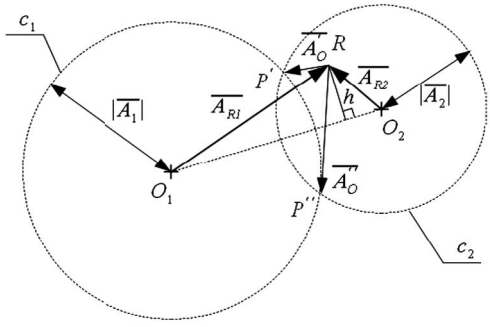

Fig. 3. Graphical solution of Eq. (4). Example.

vectors $\bar{U}'_O$ and $\bar{U}''_O$ and changing of diameter circles c_1, c_2 in the graphical approach.

Both reconstructed vectors $\bar{U}'_O$ and $\bar{U}''_O$ have their origin points in point R and end in P' and P'', respectively, which are located symmetrically with respect to straight line O_1O_2. In general case the point R is located aside of the straight line O_1O_2 and points P' and P'' are situated always symmetrically to O_1O_2. Therefore, one of both vectors $\bar{U}'_O$ and $\bar{U}''_O$ will differ in their length and the longest will always cross the O_1O_2. This circumstance can be used for an unambiguous reconstruction of the object vector $\bar{U}_O$. Suppose we can make sure that the object complex amplitude $\bar{U}'_O$ would not cross O_1O_2 straight line during the sequence of experiments because of amplitude restriction of its magnitude $|\bar{U}_O|$. Then after calculation of amplitudes $\bar{U}'_O$ and $\bar{U}''_O$ with Eq. (2) we could take the smallest value from $\bar{U}'_O$ and $\bar{U}''_O$. It will be the correct initially restricted object complex amplitude. After it the appropriate phase can be calculated with Eq. (4). If the maximum amplitude of object complex value is not restricted, we only estimate that the correct object value is among the solutions of $\bar{U}'_O$ and $\bar{U}''_O$, which are found analytically. But it is not possible to use this method for choosing the right initial object complex value.

The amplitude restriction of object wave $|\bar{U}_O|$, i.e., a limitation of the dynamic range of the object amplitude can be the solution of the ambiguity problem. The distance h between point R and O_1O_2 determines the maximum magnitude $U_{O,\max}$ of the complex object wave U_O. It can be calculated by the expression Eq. (5):

$$h = A_{O,\max} = 2\frac{|S_{\Delta O_1 R O_2}|}{|\bar{U}_{R1} - \bar{U}_{R2}|} = \frac{|\bar{U}_{R1} \times \bar{U}_{R2}|}{|\bar{U}_{R1} - \bar{U}_{R2}|} = \frac{|\bar{U}_{R1}||\bar{U}_{R2}||\sin(\delta_R)|}{\sqrt{|\bar{U}_{R1}|^2 + |\bar{U}_{R2}|^2 - 2|\bar{U}_{R1}||\bar{U}_{R2}|\cos(\delta_R)}}. \quad (5)$$

The limitation of the object wave amplitude can be carried out by attenuating illumination intensity I_{ill} of object specimen in the object arm if it exceeds the maximum squired object amplitude $I_{\text{ill}} > |U_{O,\max}|^2$.

4. Numerical Example

In this section we present simulations of the reconstruction process. The experimental interferometric setup, which can be used for the experiment, is schematically presented in Fig. 4. It is based on the modified Mach–Zendler interferometer, which was proposed in [3].

Linearly polarized at 45° the laser beam is spited into reference and object arms by beam splitter BS1. Each arm has a similar $4f$ imaging system with common L2 lens combined by beam splitter BS2. The imaging system in the object arm consists of micro-objective MO and Lens L2. It images the object plane onto intermediate image plane Im1. The system L1, L2 in the reference arm acts as a beam

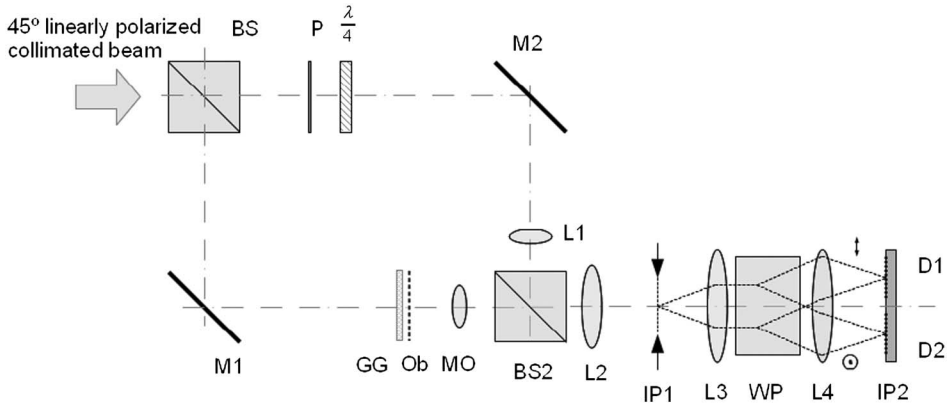

Fig. 4. Mach–Zehnder interferometric setup for two-step PSI. BS1, BS2, beam splitters; $\lambda/4$, quarter-wave plate; P, polarizer; M1, M2, mirrors; GG, ground glass; Ob, object; D1, D2, detectors; MO, micro-objective; L1–L4 , lenses; WP, Wollaston prism; IP1, IP2, imaging planes.

expander. Image plane Im2 of detectors D1 and D2 is optically conjugated with the Im1 image plane by the $4f$ imaging system containing L3 and L4 lenses. The Wollaston prism WP splits both beams from the reference and object arm in two polarizing components. Vertical polarizing components of both arms will reach detector D1 while horizontal polarizing components will be directed to the D2. Because of phase shifting at $\pi/2$ between two components, which is introduced by a quarter-wave plate in the reference arm, two interferograms will be different, namely they will correspond to the two-step phase-shifting interferograms recorded simultaneously. The orientation of polarizer P will affect the amplitude ratio of these orthogonal polarizing components. In other words, the position of polarizer P determines the amplitude ratio of both reference waves $|U_{R1}|/|U_{R2}|$.

In [2] both interference intensities are captured by two different regions of the single CCD. In our case we speak about two intended detectors D1 and D2 for capturing of different interference patterns.

The ground glass GG in the object arm is introduced for demonstrating the method's ability of restoring arbitrary phase distributions. Behind the ground glass the signal with arbitrary phase distribution and homogeneous amplitude undergoes the amplitude modulation by the amplitude object mask Ob. Actually the object may be any medium preserving the polarization of the illumination light.

Next we consider the algorithm that simulates the presented interferometer (Fig. 4). The algorithm consists of two parts. In the first part the two interferograms I_1 and I_2 are simulated. Then the reconstruction process of the object field is carried out in the detector image planes Im2.

At first we simulate the ground glass by generating a complex field with arbitrary phase and homogeneous amplitude. We suppose that behind the ground glass the amplitude of the wave is modulated by an object mask. This mask attenuates the amplitude according to the two-dimensional transmission chart presented in Fig. 5(a). The attenuation of the amplitude object ranges from 0 to 1 linearly and it carries weak deviations in the shape of the inscription "2-Step Phase-shifting Interferometry". Such artificial composite object signal can to expose the ability of the method by each possible phase and amplitude.

In the next step the reference waves U_{R1} and U_{R2} are calculated. They are the plane waves with

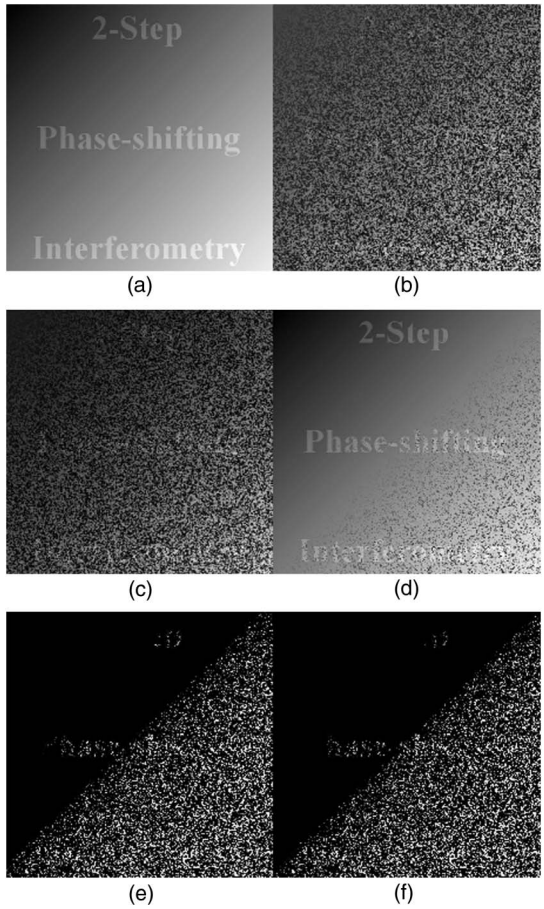

Fig. 5. Simulation results. (a) Amplitude object; (b), (c) interferograms I_1, I_2 accordingly; (d) reconstructed amplitude of object wave; (e) error regions by recovering object amplitude; (f) error regions by recovering object phase.

constant amplitude and phase. The amplitude ratio $|U_{R1}|/|U_{R2}|$ is taken to be equal to 0.5, which can be reached if the polarizer P is set under an appropriate angle. The phase difference between the reference waves determined by the $\lambda/4$ plate is $\delta_R = \pi/2$. Next the interferograms I_1 and I_2 are computed with given object and reference fields at both detectors. The reconstruction process is carried out with the analytical expressions [Eq. (2) and (3)]. The result is presented in Fig. 5.

The reconstructed object amplitude [Fig. 5(d)] is not correctly reconstructed in all regions of the image. The bottom right half of the field is distorted with dark spots. These regions have the value of the second solution of quadratic equation [Eq. (2)]. The reconstruction error occurs if object signal magnitude exceeds the some defined value $U_{O,\max} = 0.45$ estimated with Eq. (5). The error map [Fig. 5(e)] shows the reconstruction error regions. White spots depict the error regions if object wave magnitude exceeded $U_{O,\max}$ value. The presented simulation demonstrates the suggested method and illustrates the limitations for the reconstruction of object signal A_O by restriction of the object magnitude $|U_O| < U_{O,\max}$.

5. Conclusion

An analytical generalization of two-step phase-shifting interferometry was proposed. The generalization consists in the independence on the reference wave amplitudes. In the second section the analytical expressions for the reconstruction amplitude and phase are shown and discussed. Practically both reference waves can have arbitrary phase and amplitudes. The investigation of the method with a graphical vector approach in Section 3 shows that not all values can be reconstructed correctly. The condition for accurate reconstruction is the restriction of the object signal in the magnitude [Eq. (5)]. The simulation demonstrated in the Section 4 confirms the results of Section 3.

Appendix A

Estimation of object intensity I_O

$$\begin{cases} I_1 = I_{R1} + I_O + 2\sqrt{I_{R1}}\sqrt{I_O}\cos(\varphi_{R1} - \varphi_O) \\ I_2 = I_{R2} + I_O + 2\sqrt{I_{R2}}\sqrt{I_O}\cos(\varphi_{R2} - \varphi_O) \end{cases}.$$

At first we introduce the new variables:

$$\varphi_{R1} - \varphi_O = x; \qquad \varphi_{R2} - \varphi_{R1} = d; \qquad I_1 - I_{R1} = J_1; \qquad I_2 - I_{R2} = J_2.$$

In the next step the cos-factors should be expressed:

$$\begin{cases} 2\sqrt{I_{R1}}\sqrt{I_O}\cos(x) = J_1 - I_O \\ 2\sqrt{I_{R2}}\sqrt{I_O}\cos(x+d) = J_2 - I_O \end{cases},$$

$$\begin{cases} \cos(x) = \frac{J_1 - I_O}{2\sqrt{I_{R1}I_O}} \\ \cos(x+d) = \frac{J_2 - I_O}{2\sqrt{I_{R2}I_O}} \end{cases}.$$

Last derivation could be performed assuming $I_{R1} > 0$; $I_{R2} > 0$; $I_O > 0$.

All intensities are always positive. The cases where one or two reference waves have zero intensity are not considered. If object intensity I_O is equal to zero, it can cause the uncertainty "0/0" analytically in the last two equations. In this case the calculation of the phase of zero-amplitude object wave does not make sense.

After representation $\cos(x) = \cos((x + d/2) - d/2)$ for the first equation and $\cos(x+d) = \cos((x + d/2) + d/2)$ for the second equation we get

$$\begin{cases} \cos\left(\left(x + \frac{d}{2}\right) - \frac{d}{2}\right) = \frac{J_1 - I_O}{2\sqrt{I_{R1}I_O}} \\ \cos\left(\left(x + \frac{d}{2}\right) + \frac{d}{2}\right) = \frac{J_2 - I_O}{2\sqrt{I_{R2}I_O}} \end{cases},$$

$$\begin{cases} \cos(d/2)\cos(x+d/2) + \sin(d/2)\sin(x+d/2) = \frac{J_1 - I_O}{2\sqrt{I_{R1}I_O}} \\ \cos(d/2)\cos(x+d/2) - \sin(d/2)\sin(x+d/2) = \frac{J_2 - I_O}{2\sqrt{I_{R2}I_O}} \end{cases}.$$

Next we get the sum and difference of the previous equations

$$\begin{cases} 2\cos(d/2)\cos(x + d/2) = \frac{J_1 - I_O}{2\sqrt{I_{R1}I_O}} + \frac{J_2 - I_O}{2\sqrt{I_{R2}I_O}} \\ 2\sin(d/2)\sin(x + d/2) = \frac{J_1 - I_O}{2\sqrt{I_{R1}I_O}} - \frac{J_2 - I_O}{2\sqrt{I_{R2}I_O}} \end{cases},$$

$$\begin{cases} \cos(x + d/2) = \frac{J_1 - I_O}{4\cos(d/2)\sqrt{I_{R1}I_O}} + \frac{J_2 - I_O}{4\cos(d/2)\sqrt{I_{R2}I_O}} \\ \sin(x + d/2) = \frac{J_1 - I_O}{4\sin(d/2)\sqrt{I_{R1}I_O}} - \frac{J_2 - I_O}{4\sin(d/2)\sqrt{I_{R2}I_O}} \end{cases},$$

$$d \neq 0; \qquad d \neq \pi.$$

The last step can be done if the phase difference between two reference waves is not 0 and 180 degrees. The same limitation can be found in [5]. Next we use Pythagorean trigonometric identity for sine and cosine of the last equation set and then we solve the brackets:

$$1 = \left[\frac{J_1 - I_O}{4\cos(d/2)\sqrt{I_{R1}I_O}} + \frac{J_2 - I_O}{4\cos(d/2)\sqrt{I_{R2}I_O}}\right]^2 + \left[\frac{J_1 - I_O}{4\sin(d/2)\sqrt{I_{R1}I_O}} - \frac{J_2 - A^2}{4\sin(d/2)\sqrt{I_{R2}I_O}}\right]^2,$$

$$16I_O = \left[\frac{J_1 - I_O}{\cos(d/2)\sqrt{I_{R1}}} + \frac{J_2 - I_O}{\cos(d/2)\sqrt{I_{R2}}}\right]^2 + \left[\frac{J_1 - I_O}{\sin(d/2)\sqrt{I_{R1}}} - \frac{J_2 - I_O}{\sin(d/2)\sqrt{I_{R2}}}\right]^2,$$

$$16I_O = \frac{(J_1 - I_O)^2}{\cos^2(d/2)I_{R1}} + \frac{2(J_1 - I_O)(J_2 - I_O)}{\cos^2(d/2)\sqrt{I_{R1}I_{R2}}} + \frac{(J_2 - I_O)^2}{\cos^2(d/2)I_{R2}} + \frac{(J_1 - I_O)^2}{\sin^2(d/2)I_{R1}} - \frac{2(J_1 - I_O)(J_2 - I_O)}{\sin^2(d/2)\sqrt{I_{R1}I_{R2}}} + \frac{(J_2 - I_O)^2}{\sin^2(d/2)I_{R2}},$$

$$16I_O = \frac{(J_1 - I_O)^2\sin^2(d/2) + \cos^2(d/2)(J_1 - I_O)^2}{\cos^2(d/2)\sin^2(h)I_{R1}} + \frac{2(J_1 - I_O)(J_2 - I_O)\sin^2(d/2) - 2(J_1 - I_O)(J_2 - I_O)\cos^2(d/2)}{\cos^2(d/2)\sin^2(d/2)\sqrt{I_{R1}I_{R2}}} + \frac{(J_2 - I_O)^2\sin^2(d/2) + (J_2 - I_O)^2\cos^2(d/2)}{\cos^2(d/2)\sin^2(d/2)I_{R2}},$$

$$16I_O = \frac{4(J_1 - I_O)^2}{\sin^2(d)I_{R1}} - \frac{8\cos(d)(J_1 - I_O)(J_2 - I_O)}{\sin^2(d)\sqrt{I_{R1}I_{R2}}} + \frac{4(J_2 - I_O)^2}{\sin^2(d)I_{R2}},$$

$$4I_O = \frac{(J_1 - I_O)^2}{\sin^2(d)I_{R1}} - \frac{2\cos(d)(J_1 - I_O)(J_2 - I_O)}{\sin^2(d)\sqrt{I_{R1}I_{R2}}} + \frac{(J_2 - I_O)^2}{\sin^2(d)I_{R2}}.$$

After we opened brackets with object intensity I_O we get the following quadratic equation:

$$4\sin^2(d)I_{R1}I_{R2}I_O = (J_1 - I_O)^2 I_{R2} - 2\cos(d)(J_1 - I_O)(J_2 - I_O) \times \sqrt{I_{R1}I_{R2}} + (J_2 - I_O)^2 I_{R1}$$

$$4\sin^2(d)I_{R1}I_{R2}I_O = (J_1^2 - 2J_1I_O + I_O^2)I_{R2} - 2\cos(d)(J_1J_2 - (J_2 + J_1) \times I_O + I_O^2)\sqrt{I_{R1}I_{R2}} + (J_2^2 - 2J_2I_O + I_O^2)I_{R1}$$

$$4\sin^2(d)I_{R1}I_{R2}I_O = J_1^2I_{R2} - 2J_1I_{R2}I_O + I_{R2}I_O^2 - 2\cos(d)J_1J_2\sqrt{I_{R1}I_{R2}} + 2\cos(d)(J_2 + J_1)\sqrt{I_{R1}I_{R2}}I_O - 2\cos(d)\sqrt{I_{R1}I_{R2}}I_O^2 + J_2^2I_{R1} - 2J_2I_{R1}I_O + I_{R1}I_O^2$$

$$\left[I_{R1} + I_{R2} - 2\cos(d)\sqrt{I_{R1}I_{R2}}\right]I_O^2 + \left[2\cos(d)(J_2 + J_1)\sqrt{I_{R1}I_{R2}} - 2J_1I_{R2} - 2J_2I_{R1} - 4\sin^2(d)I_{R1}I_{R2}\right]I_O + J_1^2I_{R2} - 2\cos(d)J_1J_2\sqrt{I_{R1}I_{R2}} + J_2^2I_{R1} = 0$$

Appendix B

Estimation of object phase φ_O

$$\begin{cases} I_1 - I_{R1} + I_O = 2\sqrt{I_{R1}I_O}\cos(\varphi_{R1} - \varphi_O) \\ I_2 - I_{R2} + I_O = 2\sqrt{I_{R2}I_O}\cos(\varphi_{R2} - \varphi_O) \end{cases},$$

$$\begin{cases} \cos(\varphi_{R1} - \varphi_O) = \frac{I_1 - I_{R1} + I_O}{2\sqrt{I_{R1}I_O}} \\ \cos(\varphi_{R2} - \varphi_O) = \frac{I_2 - I_{R2} + I_O}{2\sqrt{I_{R2}I_O}} \end{cases}.$$

In order to keep the solution diversity of the cosine function we have to place the $\pm$ sign:

$$\begin{cases} \varphi_{R1} - \varphi_O = \pm\arccos\left(\frac{I_1 - I_{R1} + I_O}{2\sqrt{I_{R1}I_O}}\right) \\ \varphi_{R2} - \varphi_O = \pm\arccos\left(\frac{I_2 - I_{R2} + I_O}{2\sqrt{I_{R2}I_O}}\right) \end{cases},$$

$$\begin{cases} \varphi_O = \varphi_{R1} \pm \arccos\left[\frac{I_1 - I_{R1} + I_O}{2\sqrt{I_{R1}I_O}}\right] \\ \varphi_O = \varphi_{R2} \pm \arccos\left[\frac{I_2 - I_{R2} + I_O}{2\sqrt{I_{R2}I_O}}\right] \end{cases}.$$

The work is funded by the Thüringer Ministerium für Bildung Wissenschaft und Kunst through the

Graduate Schools OMITEC and Green Photonics (TMBWK, FKZ: PE 104-1-1; FKZ: B514-10062; FKZ: E715-10064), the German "Bundesministerium für Bildung und Forschung" (BMBF) within the program "Spitzenforschung und Innovation in den neuen Ländern (PROSIN)" and the project "Kompetenzdreieck Optische Mikrosysteme—OptiMi II", (FKZ: 16SV5473). D.-P. Kelly acknowledges support from Carl Zeiss Foundation (FKZ: 21-0563-2.8/121/1).

References

1. N. T. Shaked, Y. Zhu, M. T. Rinehart, and A. Wax, "Two-step-only phase-shifting interferometry with optimized detector bandwidth for microscopy of live cells," Opt. Express **17**, 15585–15591 (2009).
2. P. Gao, B. Yao, I. Harder, J. Min, R. Guo, J. Zheng, and T. Ye, "Parallel two-step phase-shifting digital holograph microscopy based on a grating pair," J. Opt. Soc. Am. A **28**, 434–440 (2011).
3. N. T. Shaked, M. T. Rinehart, and A. Wax, "Dual-interference-channel quantitative-phase microscopy of live cell dynamics," Opt. Lett. **34**, 767–769 (2009).
4. P. Gao, B. Yao, J. Min, R. Guo, J. Zheng, T. Ye, I. Harder, V. Nercissian, and K. Mantel, "Parallel two-step phase-shifting point-diffraction interferometry for microscopy based on a pair of cube beamsplitters," Opt. Express **19**, 1930–1935 (2011).
5. J. Min, B. Yao, P. Gao, R. Guo, J. Zheng, and T. Ye, "Parallel phase-shifting interferometry based on Michelson-like architecture," Appl. Opt. **49**, 6612–6616 (2010).
6. Y. Awatsuji, A. Fujii, T. Kubota, and O. Matoba, "Parallel three-step phase-shifting digital holography," Appl. Opt. **45**, 2995–3002 (2006).
7. Y. Awatsuji, T. Tahara, A. Kaneko, T. Koyama, K. Nishio, S. Ura, T. Kubota, and O. Matoba, "Parallel two-step phase-shifting digital holography," Appl. Opt. **47**, D183–D189 (2008).
8. M. A. Araiza-Esquivel, L. Martinez-León, B. Javidi, P. Andrés, J. Lancis, and E. Tajahuerce, "Single-shot color digital holography based on the fractional Talbot effect," Appl. Opt. **50**, B96–B101 (2011).
9. P. Guo and A. J. Devaney, "Digital microscopy using phase-shifting digital holography with two reference waves," Opt. Lett. **29**, 857–859 (2004).
10. C.-S. Guo, L. Zhang, H.-T. Wang, J. Liao, and Y. Y. Zhu, "Phase-shifting error and its elimination in phase-shifting digital holography," Opt. Lett. **27**, 1678–1679 (2002).
11. T. Nomura and M. Imbe, "Single-exposure phase-shifting digital holography using a random phase reference wave," Opt. Lett. **35**, 2281–2283 (2010).
12. J. Liu, T. Poon, Gu. Jhou, and P. Chen, "Comparison of two-, three-, and four-exposure quadrature phase-shifting holography," Appl. Opt. **50**, 2443–2450 (2011).
13. X. F. Meng, L. Z. Cai, X. F. Xu, X. L. Yang, X. X. Shen, G. Y. Dong, and Y. V. Wang, "Two-step phase-shifting interferometry and its application in image encryption," Opt. Lett. **31**, 1414–1416 (2006).
14. J. P. Liu and T. C. Poon, "Two-step-only quadrature phase-shifting digital holography," Opt. Lett. **34**, 250–252 (2009).
15. G. L. Chen, C. Y. Lin, H. F. Yao, M. K. Kuo, and C. C. Chang, "Wave-front reconstruction without twin-image blurring by two arbitrary step digital holograms," Opt. Express **15**, 11601–11607 (2007).
16. W. Pan, W. Lu, Y. Zhu, and Ji. Wang, "One-shot in-line digital holography based Hilbert phase-shifting," Chin. Opt. Lett. **7**, 1–4 (2009).
17. M. Servin, J. C. Estrada, and J. A. Quiroga, "The general theory of phase shifting algorithms," Opt. Express **17**, 21867–21881 (2009).
18. J. Vargas, J. A. Quiroga, T. Belenguer, M. Servín, and J. C. Estrada, "Two-step self-tuning phase-shifting interferometry," Opt. Express **19**, 638–648 (2011).
19. C. Meneses-Fabian and U. Rivera-Ortega, "Phase-shifting interferometry by wave amplitude modulation," Opt. Lett. **36**, 2417–2419 (2011).